

Observation of dipolar transport in one-dimensional photonic lattices

Camilo Cantillano · Luis Morales-Inostroza · Bastián Real · Santiago Rojas-Rojas · Aldo Delgado · Alexander Szameit · Rodrigo A. Vicencio

Received: date / Accepted: date

Abstract We experimentally study the transport properties of dipolar and fundamental modes on one dimensional (1D) coupled waveguide arrays. By carefully modulating a wide optical beam, we are able to effectively excite dipolar or fundamental modes to study discrete diffraction (single-site excitation) and gaussian beam propagation (multi-site excitation plus a phase gradient). We observe that dipolar modes experience a larger spreading area due to an effective larger coupling constant, which is found to be more than two times larger than the one for fundamental modes. Additionally, we study the effect of non-diagonal disorder and find that while fundamental modes are already trapped on a weakly disorder array, dipoles are still able to propagate across the system.

Keywords Photonic lattices · Waveguide arrays · Wave propagation · Integrated optics

1 Introduction

Waveguide arrays and photonic lattices are an important field of study where many fundamental and applied

problems can be investigated in a rather simple configuration [1,2]. Most of the theoretical and experimental efforts have been focused on studying transport and localization properties in various contexts, such as complex beam steering [3,4,5], Bloch oscillations [6,7,8], dynamic localization [9,10], relativistic emulations [11], discrete solitons [12,13,14], and many more. Recently, even the absence of transport and linear localization in complex lattice geometries was investigated [15,16,17,18,19,20].

Importantly, almost all previous works have considered single-mode waveguides only. This somehow reduces the complexity of the studied problem, allowing a more direct verification of theoretical results on simpler experimental setups. But, optical waveguides could also host higher order modes. Their excitation could promote richer dynamics and new interesting phenomena, as it has been suggested for cold-atoms loaded in optical potentials [21,22,23,24] (in that context, dipolar modes are known as p-modes). However, in general, a precise excitation of different modes or complex spatial structures may be simpler using light than atoms [15], as we will show along this work.

In this work, we present a first systematic study on the diffraction properties of dipolar modes in coupled waveguide arrays. We find that dipoles form another first tight-binding band, that is fundamentally distinct from the higher-order bands of continuous periodical systems [25]. Our waveguide arrays are fabricated using a very precise femtosecond-laser technique [26], which produces micrometer waveguides disposed on a given two-dimensional transversal pattern. Light propagating on these waveguides is well trapped in space, allowing a theoretical description based on coupled-mode theory, due to the weak coupling interaction between neighboring waveguides. By using a green laser beam and

Camilo Cantillano · Luis Morales-Inostroza · Bastián Real · Rodrigo A. Vicencio
Departamento de Física, MSI-Nucleus on Advanced Optics, and Center for Optics and Photonics (CEFOP), Facultad de Ciencias, Universidad de Chile, Santiago, Chile
E-mail: rvicencio@uchile.cl

Santiago Rojas-Rojas · Aldo Delgado
Center for Optics and Photonics and MSI-Nucleus on Advanced Optics, Universidad de Concepción, Casilla 160-C, Concepción, Chile

Alexander Szameit
Institute for Physics, University of Rostock, Albert-Einstein-Strasse 23, 18059 Rostock, Germany

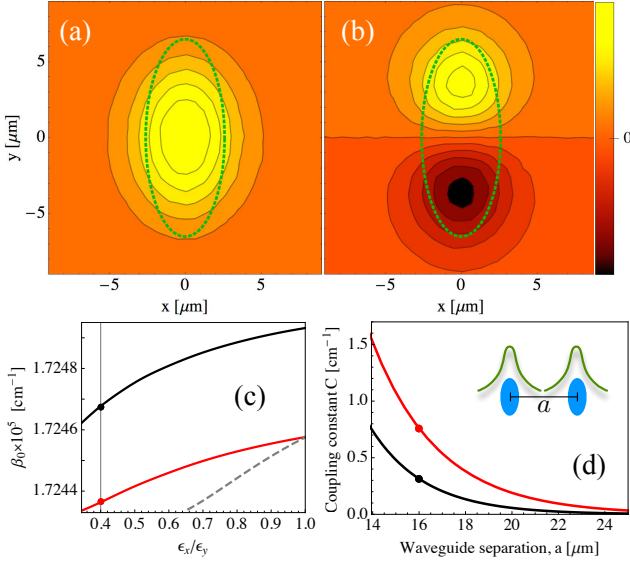


Fig. 1 Waveguide modes and their constants. **a** Fundamental and **b** dipolar mode profiles of an elliptical waveguide (dotted ellipses indicate the waveguide profile). **c** Solutions diagram in terms of the waveguide geometry ϵ_x/ϵ_y and the longitudinal propagation constant β_0 . **d** Coupling constants versus waveguide separation. In **c** and **d** fundamental and dipolar modes are shown in black and red color, respectively.

a modulation setup, we are able to effectively excite fundamental and dipolar modes, and study their dynamical properties in ordered as well as in disordered waveguide lattices [27].

2 Waveguide modes

A single-mode waveguide could become multimode when reducing the laser wavelength, or when increasing its cross-section or refractive index contrast [28, 29]. A first excited mode is denominated “dipolar” LP11 mode [30], which can have an horizontal or vertical distribution, depending on the particular waveguide geometry. The experimental excitation of higher-order modes has already been reported in Ref. [31] for highly elliptical two-dimensional waveguides [26], although a systematic study in the context of weakly coupled systems is still elusive.

The analytical treatment for finding the modes of elliptical waveguides is not trivial [32], essentially due to their geometry and complex refractive index profiles. Therefore, we implement a numerical finite-difference method to find the propagating modes of our elliptical waveguides of geometry $\epsilon_x \times \epsilon_y = 5.2 \text{ }\mu\text{m} \times 13 \text{ }\mu\text{m}$, excited using a green laser of 532 nm. Waveguide parameters were tuned in order to match our experimental observations, using a bulk fused-silica index $n_0 = 1.46$ and a maximum index contrast of $\Delta n = 0.73 \times 10^{-3}$. [This is

obtained by fitting the experimental index profiles from Ref. [26], and constructing a continuous index gradient function, where ϵ_x and ϵ_y describe the widths of the ellipse shown in Figs. 1(a) and (b)]. We look for modes of a single waveguide and find that, in our highly elliptical regime ($\epsilon_x/\epsilon_y = 0.40$), there are only two possible solutions: the fundamental mode sketched in Fig. 1(a) and the vertical dipolar mode shown in Fig. 1(b) [corresponding to dots shown in Fig. 1(c)]. We notice that the fundamental mode is well trapped at the waveguide center, while the dipolar mode presents a more extended tail in the upper and lower region, with zero amplitude at the center.

By tuning the ratio ϵ_x/ϵ_y , we find the possible solutions as a function of their longitudinal propagation constant β_0 , as shown in Fig. 1(c). We find that an additional horizontally oriented dipolar mode appears, as shown by a dashed line in Fig. 1(c). This occurs when the waveguide geometry tends to a circular limit ($\epsilon_x/\epsilon_y = 1$), where both, horizontal and vertical, dipolar modes converge and degenerate.

Following the method described in Ref. [27], we computed the horizontal coupling coefficients for fundamental and dipolar modes, for two identical waveguides separated –center to center– by a given distance a [see Fig. 1(d)]. First of all, we observe a typical exponential decaying tendency for the coupling constant of both modes [26, 31]. Then, we clearly see that the dipolar horizontal coupling is always larger due to the more extended dipole tail. As an example, for a distance $a = 16 \text{ }\mu\text{m}$, the couplings are $C^f = 0.314 \text{ cm}^{-1}$ and $C^d = 0.760 \text{ cm}^{-1}$, for the fundamental (f) and dipolar (d) modes, respectively [as indicated by dots in Fig. 1(d)]. [It is important to mention that in the configuration explored along this work (i.e., vertically oriented elliptical waveguides), there is no coupling between fundamental and dipolar modes. This is due to an exact cancellation of the superposition integral for any waveguide separation.]

3 Transport on a 1D lattice

We focus on a one-dimensional array of identical elliptical waveguides, as shown in Fig. 2(a) [each white region corresponds to the experimental propagating profile, after white-light illumination]. In this configuration, light trapped at each site of the array interacts only weakly with their surrounding via nearest-neighbor interactions. We describe the dynamics across the lattice using a set of coupled-mode equations [1, 2, 33],

$$-i \frac{d\psi_n^j}{dz} = \beta_0^j \psi_n^j + \left(C_{n+1}^j \psi_{n+1}^j + C_n^j \psi_{n-1}^j \right), \quad (1)$$

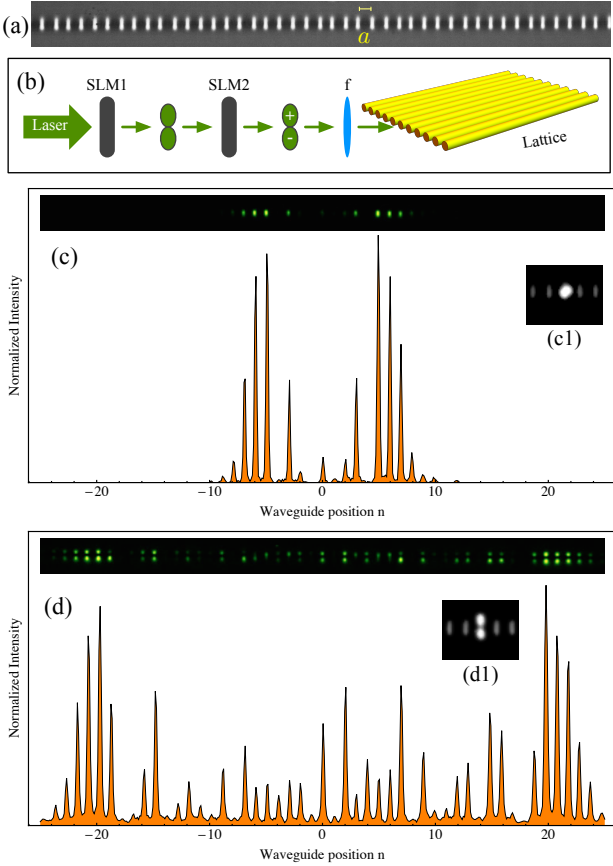


Fig. 2 Discrete diffraction. **a** Microscope image at the output facet of an ordered 1D photonic lattice. **b** Experimental setup. Discrete diffraction for a single-site **c** fundamental and **d** dipolar mode excitations, using the input profile shown in **c1** and **d1**, respectively. In **c** and **d** an output facet image (top) and an integrated transversal profile (center) are shown.

where ψ_n^j describes the amplitude of the optical field at the n th-site, for the fundamental ($j = f$) or dipolar ($j = d$) modes, while paraxially propagating along the longitudinal coordinate z . The coefficients β_0^j describe the waveguide longitudinal propagation constants, while the coefficients C_n^j correspond to the horizontal coupling coefficients between sites n and $n - 1$.

We start our study considering an homogenous ordered lattice such that $C_n^j = C^j$. When injecting light on a single lattice site, a well-known pattern is observed after evolution, the so-called discrete diffraction [1, 2]. Its main feature is to concentrate the energy not at the center (as in continuous diffraction), but at the outside external lobes. This linear problem has a formal analytical solution: $\psi_n^j(z) = \psi_0^j i^n J_n(2C^j z)$, where J_n is the Bessel function of order n . This pattern is considered as a main signature for a discrete optical system, when experiencing first band dynamics.

To experimentally study this, we fabricate an ordered lattice of 81 waveguides [see Fig. 2(a)] with a lat-

tice constant of $a = 16 \mu\text{m}$, on a $L = 10 \text{ cm}$ long fused silica chip (the geometrical shape of every waveguide corresponds to a super-gaussian of third order, with a cross section of about $4 \times 13 \mu\text{m}^2$ [34]). We study linear propagation using an experimental setup based on a sequence of two Spatial Light Modulators (SLMs) as sketched in Fig. 2(b): we first use a transmission Holoeye LC2012 SLM (SLM1) to create an amplitude profile and, then, we modulate its phase using a reflective phase-only Holoeye PLUTO SLM (SLM2). In this way, we are able to excite a lattice injecting a modulated 532 nm laser beam on a single (or several) waveguide (s) with an input profile, as shown in Figs. 2(c1) and (d1), for fundamental and dipolar excitation, respectively. The generation of dipolar input profile requires amplitude as well as phase modulation in order to mimic the mode profile shown in Fig. 1(b). However, to obtain the right experimental mode profile is not straightforward. We first inject a basic dipolar profile and experimentally observe the output image. We look for a clear dipole profile located at any waveguide and obtain its shape. Then, we use that shape to create an image in the SLM1 as a new input profile (of course, in the SLM2 we add the respective phase). We inject this new profile in the input facet and observe again the output pattern. We repeat this process up to observing only dipoles at the output profile. This is an experimentally iterative method we developed in this work, that allows us to obtain very precise input excitations.

Figs. 2(c) and (d) show the experimentally obtained discrete diffraction patterns for both input excitations. We observe that dipolar modes experience a larger spreading area compared to a standard fundamental mode excitation. The dipolar diffraction pattern shows a very broad profile, similar to the one observed for a similar lattice but using infrared light at 800 nm [35]. Our results clearly show the possibility to excite two very different spatial light distributions by simply changing the input profile. This could be used as a switch between two distinguishable orthogonal states, considering that the coupling between fundamental and dipolar modes is always zero in this geometry, without any hybridization [23].

Propagating stationary solutions of model (1) are obtained using the plane wave (PW) ansatz $\psi_n^j(z) = \psi_0^j \exp(ik_x n a) \exp(i\beta_j z)$ [4, 5]. We find the system's longitudinal frequencies β_j as a function of the transversal wave-vector k_x : $\beta_j(k_x) = \beta_0^j + 2C^j \cos(k_x a)$. This expression defines two similar linear bands, but shifted in frequency depending on the specific coefficients. Both modes experience first-band dynamics, but in two completely independent bands. $\beta_j(k_x)$ corresponds to the dispersion relation for the lattice modes, and the deriva-

tive with respect to k_x gives the transversal discrete PW velocity

$$V_x^j/a \equiv \frac{\partial \beta_j}{\partial k_x} = -2C^j \sin(k_x a), \quad (2)$$

which becomes zero for $k_x a = m\pi$, with $m \in \mathbb{Z}$. This velocity finds a maximum $|V_x^j/a| = 2C^j$ for $k_x a = (2n+1)\pi/2$, with $n \in \mathbb{Z}$. As the linear band is bounded, there is a maximum transversal velocity determined by the coupling coefficients of each excited mode [in fact, the external propagating lobes in Fig. 2(c) and (d) propagate approximately at this maximum velocity, defining the maximum covered area for linear transport on a given lattice]. In order to test this prediction, we take advantage of the capability of our experimental setup and investigate the propagation properties of an ordered lattice by injecting a tilted gaussian beam. This gaussian profile requires to be as wider as possible in order to closely represent a PW of single wave-vector k_x . However, real setups are finite in the number of waveguides as well as in the propagation coordinate. Therefore, we implement our experiment using gaussian profiles that cover only 7 sites of the array, and adjusting the gaussian width to better match the theory (2). Using our SLM setup, we generated discretized gaussian profiles composed of fundamental or dipolar modes, as shown in Fig. 3(a). We made a fine sweep of the input tilt by varying the input phase $\phi = k_x a$ in the interval $\{0, 2\pi\}$, with step size of $\pi/60$. For both mode configurations, we took 120 output profiles at $z = L$ and computed their center of mass transversal velocity, defined as $V_c^j \equiv X_c^j/L$, where $X_c^j = an_c^j$ and $n_c^j = \sum_n n |\psi_n^j|^2 / \sum_n |\psi_n^j|^2$. We collect our experimental results in Fig. 3.

We observe a good agreement between the experimental data (dots connected by lines) and the theoretical prediction for the transversal velocity (dashed lines). We made a fit of our experimental data and the theoretical formula (2), obtaining the coupling coefficients: $C^f = 0.316 \text{ cm}^{-1}$ and $C^d = 0.761 \text{ cm}^{-1}$ (these values are almost equal to the numerical coefficients described before). In the examples shown in Fig. 3, we observe a more visible dispersion for the dipolar gaussian beam compared to the fundamental mode one. This is essentially originated due to the complexity of generating a modulated dipole gaussian profile. But, nevertheless, the center of mass velocity follows a clear sine function tendency, validating our experimental method. Additionally, considering also the discrete diffraction results, we experimentally validate the use of simple (first band) tight-binding models (1) to theoretically study dipolar excitations on 1D lattices configurations.

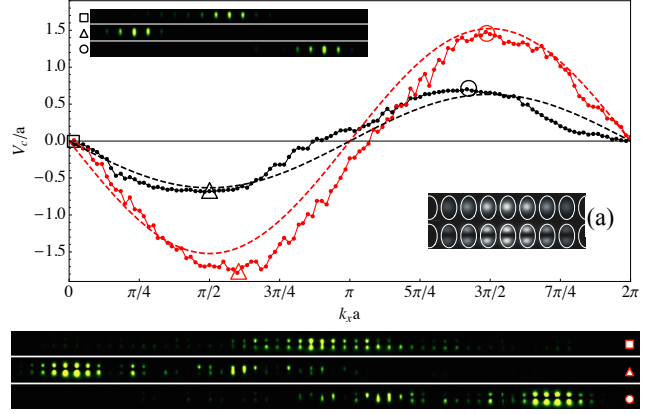


Fig. 3 Beam propagation. **a** Input profiles. Main figure: Velocity V_c/a of a discretized Gaussian beam versus the normalized transversal wavevector $k_x a$. Dots connected by lines and dashed lines correspond to the experimental and the theoretical data, respectively. Black and red color correspond to fundamental and dipolar modes. Insets show output intensity profiles corresponding to symbol positions.

4 Transport on disordered 1D lattices

Finally, we study the effect of disorder on 1D waveguide arrays, using fundamental and dipolar excitations. It is well known that disorder induces localization due to multiple destructive interference of randomly distributed scatters [36], what has been already confirmed experimentally in photonic lattices [37,38]. We fabricated eight lattices with 81 sites each, where disorder was created by randomly varying the distance between neighboring waveguides in the interval $a \in \{16 - \delta, 16 + \delta\} \mu\text{m}$, with $\delta = (0, 1, 2, 3, 4, 5, 6, 7)$. δ is defined as the spacing disorder (a larger δ implies a larger range of possible distances between neighbor waveguides, therefore an increasing degree of disorder). Our lattices, composed of identical waveguides, present only coupling (off-diagonal) disorder in model (1); i.e., the coefficients C_n^j are not constant due to the randomness in the horizontal waveguide positions [35,27] [a different waveguide separation produces a different local coupling coefficient between two neighboring waveguides, as expected from Fig.1(d)]. Figs. 4(a) and (b) show examples of an ordered ($\delta = 0$) and a disordered ($\delta = 5$) lattice. In order to have statistic, we illuminated every array in 40 different sites using single-site fundamental or dipolar mode excitations [as shown in Figs. 2(b1) and (c1)]. We obtained 40 output images for every array, and every mode, and computed the respective participation ratio $R^j \equiv (\sum |\psi_n^j|^2)^2 / \sum |\psi_n^j|^4$. We obtained an averaged value \bar{R}^j , including its standard deviation σ_R , as shown in Fig. 4(c). We observe an overall tendency to localization for both modes as the disorder strength

increases, as expected for disordered finite lattices [35, 27].

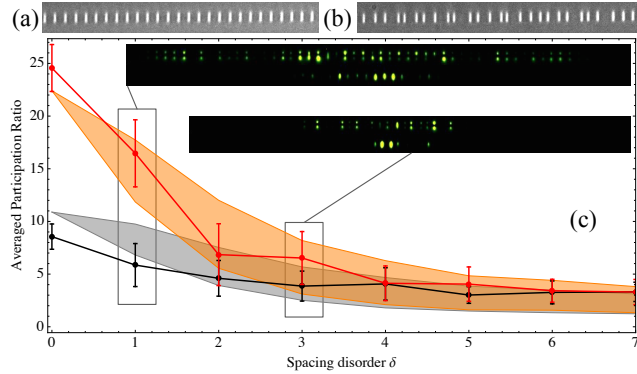


Fig. 4 Transport in disordered lattices. Microscope image at the output facet of an **a** ordered and **b** disordered one-dimensional photonic lattice. **c** Averaged participation ratio \bar{R} versus spacing disorder δ . Dots show experimental values for fundamental (black) and dipolar (red) modes (bars indicate the experimental standard deviation). The shaded regions show the numerical results for the fundamental (gray) and the dipolar (orange) modes. Insets show two examples.

We numerically integrated model (1) by considering a random distribution of coupling constants C_n^j , in the interval $\{C^j(a+\delta), C^j(a-\delta)\}$. We considered the same range of distances as in the experiments (determined by parameter δ), assuming the dependence of coupling constants presented in Fig. 1(d). We generated 100 realizations for every value of δ , and obtained the region $\bar{R}^j \pm \sigma_R$, which is shown by shaded areas in Fig. 4(c). First of all, we find a very good qualitative agreement between our experimental and numerical results, validating again the utilization of model (1) to describe the dynamics of fundamental and dipolar modes on 1D lattices. We observe that the fabricated disordered lattices rapidly conduce to localization for the fundamental mode, while there is still a good transport for dipolar propagation [see examples at $\delta = 1$]. For even stronger disorder, dipolar modes still have the opportunity to explore the lattice and disseminate the energy, while the fundamental excitation is already well localized in space. When disorder is very strong ($\delta > 4$), both modes tend to spatially localize with an almost equal averaged participation ratio of $\bar{R} \approx 3$. Although there is a strong propagation difference for zero, weak and intermediate disorder, for stronger one any input excitation will remain localized as originally predicted in Ref. [36].

5 Conclusions

In conclusion, we have theoretically and experimentally studied a 1D waveguide array by considering fundamental and dipolar mode excitations. We have shown, using single-site and gaussian beam excitations, that the spreading area is enhanced for dipolar modes in this lattice. Additionally, we have explored the effect of considering disorder on a 1D lattice and have shown that its effect is weaker for dipolar modes, although for stronger disorder both modes localize. After three different experiments, we validate the use of model (1) as a good theoretical description to study the dynamics of fundamental and dipolar modes in a first-band environment. Extension to hybrid interactions, higher dimensions, and nonlinear effects [21, 22, 23, 39, 40, 41, 42, 43] are interesting extensions to be explored in detail in the future. Our experimental results may open up a new window to perform p-orbital quantum simulations using photons. Our setup may also provide a more controllable platform for the study of exotic p-orbital phases, which have been previously suggested in the context of cold atoms in optical lattices [24].

Acknowledgements Authors want to acknowledge M. Johansson for useful discussions and U. Naether for fabricating the lattices. This work was supported in part by Programa ICM grant RC130001, FONDECYT Grant No. 1151444, the Deutsche Forschungsgemeinschaft (grant NO 462/6-1, SZ 276/7-1, SZ 276/9-1, BL 574/13-1), and the German Ministry of Education and Research (Center for Innovation Competence program, grant 03Z1HN31).

References

1. Lederer F, Stegeman G.I., Christodoulides D.N., Assanto G., Segev M., Silberberg Y. (2008) Discrete solitons in optics. *Phys. Rep.* 463: 1
2. Flach S, Gorbach A (2008) Discrete breathers – Advances in theory and applications. *Phys. Rep.* 467: 1
3. Aceves AB, De Angelis C, Trillo S, Wabnitz S (1994) Storage and steering of self-trapped discrete solitons in nonlinear waveguide arrays. *Opt. Lett.* 19: 332
4. Pertsch T, Zentgraf T, Peschel U, Brauer A, Lederer F (2002) Anomalous refraction and diffraction in discrete optical systems. *Phys. Rev. Lett.* 88: 093901
5. Eisenberg HS, Silberberg Y, Morandotti R, Aitchison JS (2000) Diffraction management. *Phys. Rev. Lett.* 85: 1863
6. Pertsch T, Dannberg P, Elfle W, Brauer A, Lederer F (1999) Optical Bloch oscillations in temperature tuned waveguide arrays. *Phys. Rev. Lett.* 83: 4752
7. Peschel U, Pertsch T, Lederer F (1998) Optical Bloch oscillations in waveguide arrays. *Opt. Lett.* 23: 1701
8. Trompeter H, Krolikowski W, Neshev DN, Desyatnikov AS, Sukhorukov AA, Kivshar YS, Pertsch T, Peschel U, Lederer F (2006) Bloch oscillations and zener tunneling in two-dimensional photonic lattices. *Phys. Rev. Lett.* 96: 053903

9. Longhi S, Marangoni M, Lobino M, Ramponi R, Laporta P, Cianci E, Foglietti V (2006) Observation of dynamic localization in periodically curved waveguide arrays. *Phys. Rev. Lett.* 96: 243901
10. Szameit A, Garanovich IL, Heinrich M, Sukhorukov AA, Dreisow F, Pertsch T, Nolte S, Tünnermann A, Longhi S, Kivshar YS (2010) Observation of two-dimensional dynamic localization of light. *Phys. Rev. Lett.* 104: 223903
11. Keil R, Zeuner JM, Dreisow F, Heinrich M, Tünnermann A, Nolte S, Szameit A (2013) The random mass Dirac model and long-range correlations on an integrated optical platform. *Nat. Commun.* 4: 1368
12. Christodoulides DN, Joseph RI (1988) Discrete self-focusing in nonlinear arrays of coupled waveguides. *Opt. Lett.* 13: 794
13. Eisenberg HS, Silberberg Y, Morandotti R, Boyd AR, Aitchison JS (1998) Discrete spatial optical solitons in waveguide arrays. *Phys. Rev. Lett.* 81: 3383
14. Fleischer JW, Segev M, Efremidis NK, Christodoulides DN (2003) Observation of two-dimensional discrete solitons in optically induced nonlinear photonic lattices. *Nature* 422: 147
15. Vicencio RA, Cantillano C, Morales-Inostroza L, Real B, Mejía-Cortés C, Weimann S, Szameit A, Molina MI (2015) Observation of Localized States in Lieb Photonic Lattices. *Phys. Rev. Lett.* 114: 245503
16. Mukherjee S, Spracklen A, Choudhury D, Goldman N, Öhberg P, Andersson E, Thomson RR (2015) Observation of a Localized Flat-Band State in a Photonic Lieb Lattice. *Phys. Rev. Lett.* 114: 245504
17. Mukherjee S, Thomson RR (2015) Observation of localized flat-band modes in a quasi-one-dimensional photonic rhombic lattice. *Opt. Lett.* 40: 5443
18. Weimann S, Morales-Inostroza L, Real B, Cantillano C, Szameit A, Vicencio RA (2016) Transport in sawtooth photonic lattices. *Opt. Lett.* 41: 2414
19. Xia S, Hu Y, Song D, Zong Y, Tang L, Chen Z (2016) Demonstration of flat-band image transmission in optically induced Lieb photonic lattices. *Opt. Lett.* 41: 1435
20. Zong Y, Xia S, Tang L, Song D, Hu Y, Pei Y, Su J, Li Y, Chen Z (2016) Observation of localized flat-band states in Kagome photonic lattices. *Optics Express* 24: 8877
21. Wu C, Bergman D, Balents L, Das Sarma S (2007) Flat Bands and Wigner Crystallization in the Honeycomb Optical Lattice. *Phys. Rev. Lett.* 88: 070401
22. Li X, Zhao E, Liu WV (2013) Topological states in a ladder-like optical lattice containing ultracold atoms in higher orbital bands. *Nat. Commun.* 4: 1523
23. Yin S, Baarsma JE, Heikkinen MOJ, Martikainen JP, Törmä P (2015) Superfluid phases of fermions with hybridized s and p orbitals. *Phys. Rev. A* 92: 053616
24. Li X, Liu W V (2016) Physics of higher orbital bands in optical lattices: a review. *Rep. Prog. Phys.* 79: 116401
25. Mandelik D, Eisenberg HS, Silberberg Y, Morandotti R, Aitchison JS (2003) Band-gap structure of waveguide arrays and excitation of floquet-bloch solitons. *Phys. Rev. Lett.* 90: 053902
26. Szameit A, Nolte S (2010) Discrete optics in femtosecond-laser-written photonic structures. *J. Phys. B: At. Mol. Opt. Phys.* 43: 163001
27. Rojas-Rojas S, Morales-Inostroza L, Naether U, Xavier GB, Nolte S, Szameit A, Vicencio RA, Lima G, Delgado A (2014) Analytical model for polarization-dependent light propagation in waveguide arrays and applications. *Phys. Rev. A* 90: 063823
28. Snyder AW, Young WR (1978) Modes of optical waveguides. *J. Opt. Soc. Am* 68: 297
29. Snyder AW, Love JD (1983) *Optical Waveguide Theory*. Chapman and Hall, New York
30. Gloge D (1971) Weakly guiding fibers. *Appl. Opt.* 10: 2252
31. Szameit A, Blömer D, Burghoff J, Pertsch T, Nolte S, Tünnermann A (2006) Hexagonal waveguide arrays written with fs-laser pulses. *Appl. Phys. B* 82: 507
32. Kumar A, Varshney RK (1984) Propagation characteristics of highly elliptical core optical waveguides: a perturbation approach. *Opt. Quantum Electron.* 16: 349
33. Marcuse D (1974) *Theory of Dielectric Optical Waveguides*. New York: Academic Press
34. Szameit A, Dreisow F, Pertsch T, Nolte S, Tünnermann A (2007) Control of directional evanescent coupling in fs laser written waveguides. *Opt. Exp.* 15: 1579
35. Naether U, Rojas-Rojas S, Martínez AJ, Stützer S, Tünnermann A, Nolte S, Molina MI, Vicencio RA, Szameit A (2013) Enhanced distribution of a wave-packet in lattices with disorder and nonlinearity. *Opt. Express* 21: 927
36. Anderson PW (1958) Absence of Diffusion in Certain Random Lattices. *Phys. Rev.* 109: 1492
37. Schwartz T, Bartal G, Fishman S, Segev M (2007) Transport and Anderson localization in disordered two-dimensional photonic lattices. *Nature* 446: 52
38. Lahini Y, Avidan A, Pozzi F, Sorel M, Morandotti R, Christodoulides DN, Silberberg Y (2008) Anderson Localization and Nonlinearity in One-Dimensional Disordered Photonic Lattices. *Phys. Rev. Lett.* 100: 013906
39. Johansson M, Sukhorukov AA, Kivshar YS (2009) Discrete reduced-symmetry solitons and second-band vortices in two-dimensional nonlinear waveguide arrays. *Phys. Rev. E* 80: 046604
40. Conforti M, De Angelis C, Akylas TR (2011) Energy localization and transport in binary waveguide arrays. *Phys. Rev. A* 83: 043822
41. Keil R, Poli C, Heinrich M, Arkinstall J, Weihs G, Schomerus H, Szameit A (2016) Universal sign control of coupling in tight-binding lattices. *Phys. Rev. Lett.* 116: 213901
42. Rose R, Richter R, Terhalle B, Imbrock J, Kaiser F, Denz C (2007) Discrete and dipole-mode gap solitons in higher-order nonlinear photonic lattices. *Appl. Phys. B* 89: 521
43. Xia S, Song D, Zong Y, Tang L, Chen Z (2015) Observation of self-trapping and rotation of higher-band solitons in two-dimensional photonic lattices. *Opt. Express* 23: 4397